CHEMISTRY
A European Journal

A Journal of
ChemPubSoc Europe

Accepted Article

Title: A Cu(II) coordination polymer based exfoliated nano-sheet inhibits □-chymotrypsin

Authors: Parthasarathi Dastidar and Koushik Sarkar

To be cited as: *Chem. Eur. J.* 10.1002/chem.201802376

Link to VoR: http://dx.doi.org/10.1002/chem.201802376

Supported by
ACES

WILEY-VCH

10.1002/chem.201802376

COMMUNICATION

WILEY-VCH

A Cu(II) Coordination Polymer Based Exfoliated Nano-sheet Inhibits α-chymotrypsin

Koushik Sarkar and Parthasarathi Dastidar*[a]

Abstract: A 2D coordination polymer derived from 5-azidoisophthalic acid (AIA) and $Cu(NO_3)_2$ was designed with the aim of modulating the activity of a digestive enzyme α-chymotrypsin (**ChT**). The coordination polymer namely $\{[Cu_{0.5}(\mu\text{-}AIA)_{0.5}(H_2O)].2H_2O\}_\alpha$ (**CP1**) was successfully synthesized and fully characterized by single crystal X-ray diffraction (SXRD). Exfoliated nano-sheet (ENS) of **CP1** was readily produced by overnight stirring of hand-ground **CP1** crystals dispersed in DMSO. ENS(CP1) was demonstrated to be acting as an inhibitor of **ChT**; as much as ~97% inhibition of **ChT** was achieved with 100 μM of ENS(CP1) using N-succinyl-L-phenylalanine-p-nitroanilide (SPNA) as substrate. Enzyme kinetics data revealed that the inhibition of **ChT** followed a competitive pathway. Enzyme assay under varying ionic strength and varying concentration of free histidine revealed that the active site His-57 participated in coordination with Cu(II) metal center of ENS(CP1) thereby preventing the substrate (SPNA) from binding with the enzyme resulting in efficient inhibition.

Coordination polymers[1] (CPs) have been exploited in many diverse fields, like gas adsorption and separation,[2] anion separation,[3] catalysis,[4] magnetism,[5] post synthetic modification[6], bio-mineralization,[7] drug delivery and healthcare applications.[8] CPs are usually synthesized via building block approach wherein organic linkers (ligands) are reacted with suitable metal centers; the resulting crystalline CPs are characterized by single crystal X-ray diffraction (SXRD) providing details of the structures at atomic resolution; virtually infinite combinations of ligands and metals offer unmatched compositional and structural diversities allowing tuneable physicochemical properties that consequently help in developing materials for such diverse applications.[2-8]

Modulating enzyme activity is important as it can provide means to control various important biological processes;[9] it can be achieved by designing artificial receptors that specifically bind to the enzyme surface or its active site thereby preventing enzyme-enzyme or enzyme-substrate binding.[10] Complex topology of enzyme surface induced by hydrophobic, electrostatic and hydrophilic residues, large interfacial area required for preventing enzyme-enzyme interactions and relatively small (in the order of a few nm) opening to the active site make the design particularly difficult. Nevertheless, nanoparticles,[11]

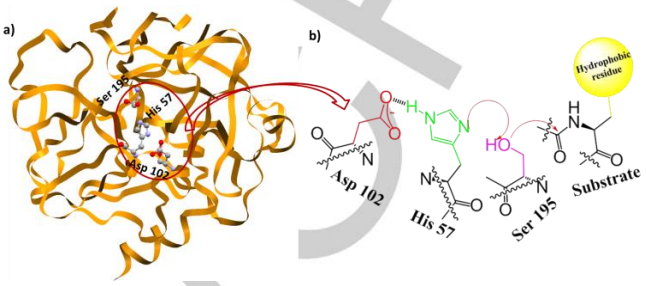

Scheme 1: a) catalytic triad and b) its mode of action in **ChT**.

dendrimers,[12] small organic molecules,[13] macro-assemblies,[14] nanotubes,[15] metal-organic complexes[16] have been used to modulate enzyme activity. The structures of CPs, on the other hand, are highly tuneable; it can offer high surface area and various contact sites such as unsaturated coordinating metal centers, periodic array of counter ions, hydrophobic or hydrophilic surface etc. to promote enzyme-CP binding. However, CPs have hitherto been exploited scarcely to modulate enzyme activity.[17]

In this communication, we have demonstrated that a 2D exfoliated nano-sheet (ENS) derived from a Cu(II) CP can indeed be accessed by design to inhibit the activity of α-chymotrypsin (**ChT**) as much as ~97 %.

Modulating the activity of **ChT** has been a popular research target as immoderate activity of **ChT** is linked with various disorders such as cystic fibrosis,[18] inflammatory arthritis[19] etc. Various materials such as dendrimers,[20] nano MoS_2,[21] nanoparticles,[22] graphene oxides,[23] carbon nanotube,[24] metal complexes,[25] calix-peptide conjugates[26] have been reported as **ChT** inhibitors.

ChT is a digestive enzyme available in the pancreatic juice. It is a serine protease that catalyses the breakdown of proteins and polypeptides. Its 3D structure is well characterized by SXRD.[27] The active site is surrounded by cationic residues such as arginine (Arg) and lysine (Lys). The so called 'catalytic triad' of the enzyme contains three residues namely Ser-195, His-57 and Asp-102. While Asp-102 holds His-57 in position via N-H···O hydrogen bonding, the lone pair of electron of the imidazole moiety of His-57 abstracts proton from the hydroxyl group of Ser-195 making it a powerful nucleophile which attacks the carbonyl of amide moiety of the substrate thereby catalysing the proteolysis process (Scheme 1). Since the active side is located within a hydrophobic pocket, it preferably catalyses the cleavage of peptide bonds having hydrophobic side chains such as phenyl alanine, tyrosine and tryptophan. It is interesting to note that the perpendicular distance from the protein surface to the imidazole N of His-57 is ~3 Å thereby making it accessible to coordination to metal center in a CP (the calculation was based on the coordinates of **ChT** retrieved from protein data bank). Thus,

[a] K. Sarkar and Prof. P. Dastidar
Department of Organic Chemistry
Indian Association for the Cultivation of Science (IACS)
2A and 2B, Raja S. C. Mullick Road
Jadavpur, Kolkata, 700032, West Bengal (India)
Fax: (+91) 33-2473-2805
E-mail: ocpd@iacs.res.in

Supporting information for this article is given via a link at the end of the document.

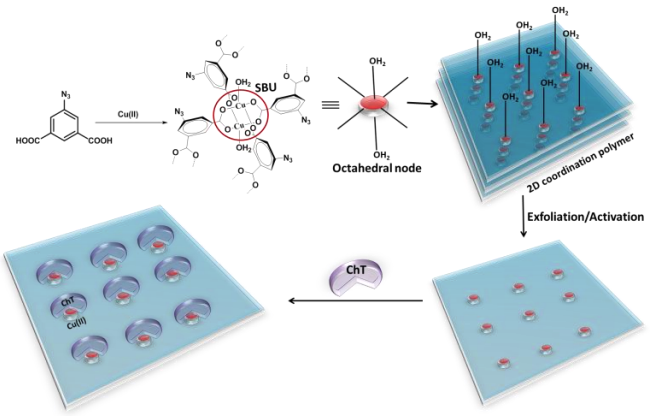

Scheme 2: Schematic representation of inhibition of ChT by activated exfoliated nano-sheet of the coordination polymer **CP1**.

periodic array of coordinatively unsaturated metal centers which can easily be envisaged in a 2D CP can effectively bind imidazole N of His-57 thereby preventing proton abstraction from Ser-195 consequently modulating the activity of **ChT** towards effective inhibition. It is also understandable that the efficiency of such metal-N coordination leading to **ChT** inhibition would be maximum in nanoscale due to large surface area. With this background, we set out our effort to design a counter ion free 2D Cu(II) CP, the ENS of which would expectedly inhibit **ChT** by accessing the coordinatively unsaturated Cu(II) metal center. For this purpose, we chose to work with an azido functionalized aromatic dicarboxylic acid ligand namely 5-azidoisophthalic acid (**AIA**) and $Cu(NO_3)_2$. The reaction between **AIA** and the Cu(II) salt is expected to produce counter ion free 2D CP via $Cu_2(COO)_4$ paddle-wheel secondary building unit (SBU). Covalently linked azido moiety being hydrophobic and non-coordinative, **AIA** moiety should provide the required hydrophobicity for effective binding with **ChT**; the coordinatively unsaturated Cu(II) center of the paddle-wheel SBU obtained after removing axially coordinated solvent molecule by mild heating may facilitate coordination with His-57 of the active site thereby effectively inhibiting the activity of **ChT** (Scheme 2). Slow evaporation of a EtOH-water (4:1) solution containing disodium **AIA** (Na_2AIA) and $Cu(NO_3)_2$ in 1:1 molar ratio resulted in X-ray quality crystals at rt. after 24 h. The isolated crystals were subjected to various physicochemical characterizations including SXRD. The space group assigned to the mounted crystal for SXRD was *P*4/nmm (tetragonal, No. 129). Analyses revealed that it was a 2D CP having a formulae $\{[Cu_{0.5}(\mu\text{-}AIA)_{0.5}(H_2O)].2H_2O\}_\alpha$ (**CP1**). In the crystal structure of **CP1**, the carboxylate moiety of **AIA** formed paddle-wheel SBU with Cu(II) – the axial positions of which were occupied by coordinated water molecules; the supramolecular architecture may best be described as corrugated 2D square grid that further packed in parallel fashion along the c-axis. 4-fold symmetry axis was located at the center of each grid and the alternating grids were occupied by solvate water and pendent azido moiety (rotationally disordered around the 4-fold axis). While one of the solvate water molecules was found to be interacting with the metal bound water of the 2D CP via O-H···O hydrogen bonding, the other solvate water molecule formed a discrete hydrogen bonded water cluster having four water molecules around the 4-fold symmetry axis (Figure 1a).

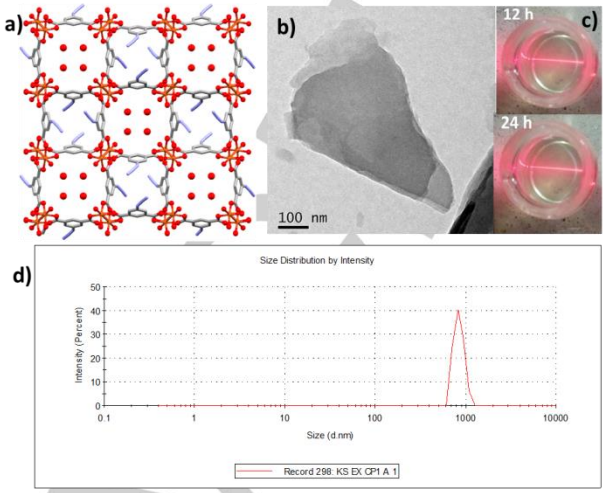

Figure 1: a) Crystal structure illustration of **CP1** displaying 2D polymeric network; b) TEM image of the nano-sheet; c) Tyndall scattering of the dispersed nano-sheets in DMSO/PBS; d) DLS trace of the suspended nano-sheets in DMSO/PBS.

Therefore, the 2D corrugated sheets were primarily held together via O-H···O hydrogen bond which, under suitable conditions, may be exfoliated to produce the targeted 2D exfoliated nano-sheets i.e. ENS(CP1). A small amount of crystals of **CP1** was hand-ground in a mortar and pestle and stirred overnight in DMSO. The resulting suspension of **CP1** in DMSO was drop casted on a carbon coated Cu grid (300 mesh) and the corresponding TEM images were recorded. 2D nano-sheets (~ 450 × 850 nm) were observed in the TEM images indicating the formation of exfoliated nano-sheets of **CP1**. AFM images of the exfoliated nano-sheets revealed that the average thickness was ~1.7 nm which was in close agreement with the value obtained from SXRD (Figure S13). Tyndall scattering of suspended nano-sheets of **CP1** both in DMSO and DMSO/Phosphate Buffered Saline (PBS) for a period of 24 h indicated good dispersion and stability of the 2D exfoliated nano-sheets (Figure S4, Supporting information). Particles having hydrodynamic diameter of ~850 nm were evident from DLS data that supported the size observed in TEM images (Figure 1b-d).

Having successfully made the exfoliated nano-sheets of **CP1**, we then undertook **ChT** activity assay to study the extent of inhibition of **ChT** activity by the nano-sheet. For this purpose, we have taken N-succinyl-L-phenylalanine-p-nitroanilide (SPNA) as a model substrate. **ChT** catalyzes the hydrolysis of the amide

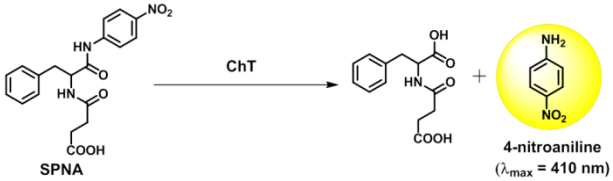

Scheme 3

linkage adjacent to phenylalanine of the colourless SPNA releasing light yellow 4-nitroaniline (Scheme 3). Thus, the progress of the catalytic reaction can be monitored by UV-vis spectroscopy.

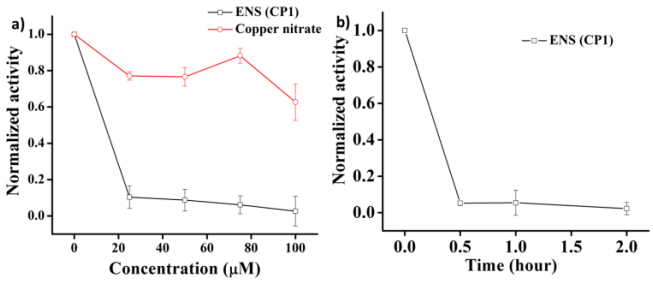

Figure 2: Normalized activity of **ChT** a) in presence of varying concentration of ENS(CP1) and copper nitrate; b) in presence of 100 μM ENS(CP1) as a function of time.

The rate of the catalytic reaction can be used to determine the extent of enzyme inhibition. The activity of free **ChT** is considered unity (100%) thereby normalizing the inhibited enzyme activity in the presence of nano-sheet keeping the incubation period of 1 h in all experiments. Prior monitoring of **ChT** activity in presence of 100 μM ENS(CP1) suggested that the inhibition of **ChT** reached a saturation level after 1 h. The enzyme activity was found to be reduced with the increase in concentration of the nano-sheet. Maximum inhibition of ~97 % was observed at a concentration of 100 μM of the nano-sheet. As a control experiment, we have carried out the assay in presence $Cu(NO_3)_2$ (100 μM) that could only inhibit up to ~37 % under identical conditions. These data clearly indicated that ENS(CP1) was able to inhibit **ChT** activity more efficiently than simple $Cu(NO_3)_2$ that corroborated well with the hypothesis based on which the current design was undertaken (see above) (Figure 2).

To provide further support that the coordinative interactions between His-57 of **ChT** and Cu(II) metal center of the nano-sheet was responsible for such inhibition of the enzyme, we carried out **ChT** activity assay in presence of varying concentration of NaCl. Since the active site of **ChT** is cationic (see above), NaCl is likely to interact strongly with the enzyme driven by electrostatic interactions. Thus, under high ionic strength, the enzyme activity is expected to be recovered. Indeed, the enzyme pre-incubated with the increasing concentration of NaCl (0-300 mM) showed a recovery of its activity from ~2% (0 mM NaCl) to ~60% (300 mM NaCl) in presence of fixed concentration of ENS(CP1) (100 μM). Interestingly, when the same experiments were performed with **ChT** pre-incubated with ENS(CP1) (100 μM), the recovery of the enzyme activity was negligible (from ~3% (0 mM NaCl) to ~15% (300 mM NaCl)). Interestingly, the activity of **ChT** pre-incubated with ENS(CP1) (100 μM) with the increasing concentration of free histidine (0-300 μM) was found to be significantly recovered (from ~5% (0 μM histidine) to ~64% (300 μM histidine)). From these data, it can be concluded that the inhibition of **ChT** was predominantly driven by blocking the active site of the enzyme via His-57-Cu(II) coordination which can be made free for substrate recognition by the addition of free histidine; the driving force behind such release of **ChT** in presence of free histidine is in most likelyhood the entropy gain (Figure 3).

To get more insight into the mode of binding of the substrate (SPNA) and inhibitor ENS(CP1) with **ChT**, enzyme kinetic studies were undertaken. Both Michaelis−Menten and mixed model kinetics (Lineweaver−Burk plot) were invoked for this purpose.[28]

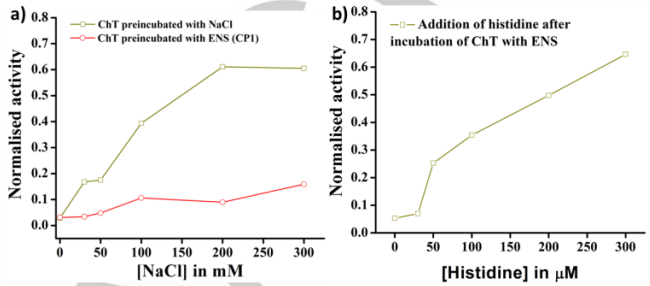

Figure 3: Normalized activity of **ChT** a) with varying ionic strength; b) with varying concentration of free histidine.

Enzyme velocity data as a function of substrate concentration at a fixed inhibitor concentration (100 μM) provided important kinetic parameters such as Michaelis−Menten constant (K_m), inhibition constants (K_i and α), catalytic constant (K_{cat}) and maximum reaction rate (V_{max}) from Lineweaver−Burk plot (**Eqn. 1**) (Supporting information).

$$\frac{1}{v} = \frac{1 + [I]/\alpha K_i}{v_{max}} + \frac{K_m(1 + [I]/K_i)}{v_{max}[s]} \quad \text{--------} \quad \text{Eqn. 1}$$

The mode of enzyme catalysis depends on the value of α.[29] When α = 1, it is a noncompetitive inhibition process wherein inhibitor does not influence enzyme-substrate binding. If α << 1, the inhibition process is via uncompetitive mode wherein inhibitor–enzyme binding causes enhanced substrate binding. In competitive mode, α >> 1 wherein enzyme-inhibitor binding significantly prevents enzyme-substrate binding. In the present study, we obtained α = 32.9 indicating competitive mode of inhibition i.e. the inhibitor-enzyme binding reduces enzyme-substrate binding. We attributed such competitive mode of inhibition to effective coordination between Cu(II) metal center of the nano-sheet with His-57 of **ChT** active site via imidazole N-Cu(II) coordination thereby preventing substrate binding (Figure 4).

The fact that the secondary structure of **ChT** did not change significantly in the presence of ENS(CP1) was confirmed from both the emission and CD spectra. Excitation of free **ChT** as well as in presence of ENS(CP1) (100 μM) in PBS at 295 nm provided a peak at 334 nm whereas denatured **ChT** (obtained by heating at 90 °C for 1.5 h) resulted in a bathochromic shift to 347 nm under identical conditions. In CD, free **ChT** in PBS showed two characteristic minima (232 and 204 nm) whereas denatured **ChT** displayed a single minima at 200 nm. The CD spectrum of **ChT** preincubated with ENS(CP1) for 1 h was found to be nearly superimposable with that obtained from free **ChT**

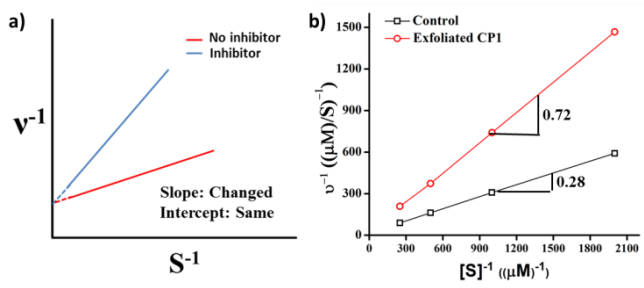

Figure 4: Competitive mode of inhibition: a) theoretical plot; b) experimental plot.

indicating that the enzyme retained its secondary structure during competitive inhibition (Figure S7, Supporting information). The data presented thus far suggest that the ENS(CP1) provided an array of coordinatively unsaturated Cu(II) metal center on the 2D nano-sheets for the enzyme to bind via His-57-Cu(II) coordination leading towards efficient inhibition. Such understanding encouraged us to study the inhibition of **ChT** using nanoparticles of **CP1**. Ball-mill grinding of **CP1** crystals resulted in nanoparticles (~170 nm) as revealed by TEM and DLS (Figure S8, S9, supporting information). It may be noted that the fits to the scattering data in DLS were not perfect as the nanoparticles were assumed to be spherical in the fit and therefore, the size of the nanoparticles inferred from DLS might be prone to error. Interestingly, **CP1** in its nanoparticle form was found to be relatively less efficient in inhibiting **ChT** (~92 %) as compared that of ENS(CP1) under identical conditions (Figure S10, Supporting information).

So far the data obtained suggested that the exfoliated nano-sheet of **CP1** could indeed be utilized to regulate the ChT activity. In order to translate such property of the nano-sheet in real-life application, it is important to evaluate its cytotoxicity. For this purpose, we carried out MTT assay on RAW 264.7 cells, a murine macrophage cell line of mice. Data revealed that the survival of the cells was >60 % at a concentration of 100 μM and ~99 % at a concentration of 25 μM. Thus, the nano-sheet of **CP1** turned out to be highly biocompatible (Figure S12, Supporting information).

To summarize - as much as ~97 % inhibition of the activity of α-chymotrypsin was achieved by exfoliated nano-sheet of a counter anion free neutral 2D Cu(II) coordination polymer **CP1** which was designed based on structural consideration of the active site of the enzyme as well as its mode of action. SXRD revealed that CP1 was indeed a 2D neutral coordination polymer wherein the axial sites of the Cu(II) metal center of $Cu_2(COO)_4$ SBU could be made available for His-57 for coordination towards effective inhibition of the enzyme. Activity assay under varying ionic strength as well as free histidine also supported this view. Enzyme kinetics suggested that the inhibition followed a competitive pathway. Most importantly, the exfoliated nano-sheet of **CP1** was also demonstrated to be biocompatible in RAW 264.7 cell line; while IC_{50} was found to be 100 μM, nearly 99 % survival of the cells was recorded at a concentration of 25 μM. The results presented herein is one of the rare examples of coordination polymer based material as efficient enzyme inhibitor and provide valuable insights towards the understanding of enzyme-coordination polymer interactions that might lead to developing organic-inorganic hybrid materials as enzyme inhibitors.

Acknowledgements

K.S thanks CSIR for research fellowship. P.D thanks DST (EMR/2016/000894) for financial support. Single crystal X-ray diffraction facility at the Department of Organic Chemistry, IACS supported by CEIB program of DBT (BT/01/CEIB/11/V/13) was used for data collection. We thank Prof. Dilip Kr. Maity, Department of Organic Chemistry, University of Calcutta for helping in DLS data collection. We thank Ms. Ivy Ghosh, Department of Inorganic Chemistry, IACS for helping in UV-Vis data collection.

Keywords: Coordination polymer • Exfoliation • α-chymotrypsin • Enzymatic modulation • Biocompatibility

Caution! Although we did not experience any problems with **AIA** and **CP1** reported in this work, azide containing compounds are potentially explosive. Therefore it should be handled with care.

[1] a) B. F. Hoskins, R. Robson, *J. Am. Chem. Soc.* **1989**, *111*, 5962-5964; b) H. Furukawa, N. Ko, Y. B. Go, N. Aratani, S. B. Choi, E. Choi, A. O. Yazaydin, R. Q. Snurr, M. O'Keeffe, J. Kim, O. M. Yaghi, *Science* **2010**, *329*, 424-428; c) S. L. James, *Chem. Soc. Rev.* **2003**, *32*, 276-288; d) P. Byrne, G. O. Lloyd, N. Clarke, J. W. Steed, *Angew. Chem. Int. Ed.* **2008**, *47*, 5761-5764.
[2] J. A. Mason, M. Veenstra, J. R. Long, *Chem. Sci.* **2014**, *5*, 32-51.
[3] R. Custelcean, *Chem. Soc. Rev.* **2014**, *43*, 1813-1824.
[4] J. Y. Lee, O. K. Farha, J. Roberts, K. I. Scheidt, S. T. Nguyen, J. T. Hupp, *Chem. Soc. Rev.* **2009**, *38*, 1450-1459.
[5] W. Zhang, R.-G. Xiong, *Chem. Rev.* **2012**, *112*, 1163-1195.
[6] Z. Wang, S. M. Cohen, *Chem. Soc. Rev.* **2009**, *38*, 1315-1329.
[7] K. Liang, R. Ricco, C. M. Doherty, M. J. Styles, S. Bell, N. Kirby, S. Mudie, D. Haylock, A. J. Hill, C. J. Doonan, P. Falcaro, *Nat. Commun.* **2015**, *6*, 7240.
[8] a) J. D. Rocca, D. Liu, W. Lin, *Acc. Chem. Res.* **2011**, *44*, 957-968; b) P. Horcajada, R. Gref, T. Baati, P. K. Allan, G. Maurin, P. Couvreur, G. Férey, R. E. Morris, C. Serre, *Chem. Rev.* **2012**, *112*, 1232-1268.
[9] D. E. Atkinson, *Ann. Rev. Biochem.* **1966**, *35*, 85-124.
[10] M. W. Peczuh, A. D. Hamilton, *Chem. Rev.* **2000**, *100*, 2479-2494.
[11] S.-H. Cha, J. Hong, M. McGuffie, B. Yeom, J. S. VanEpps, N. A. Kotov, *ACS Nano* **2015**, *9*, 9097-9105.
[12] F. Chiba, T.-C. Hu, L. J. Twyman, M. Wagstaff, *Chem. Commun.* **2008**, 4351-4353.
[13] J. W. Tilley, L. Chen, D. C. Fry, S. D. Emerson, G. D. Powers, D. Biondi, T. Varnell, R. Trilles, R. Guthrie, F. Mennona, G. Kaplan, R. A. LeMahieu, M. Carson, R.-J. Han, C.-M. Liu, R. Palermo, G. Ju, *J. Am. Chem. Soc.* **1997**, *119*, 7589-7590.
[14] H. M. Piwonski, M. Goomanovsky, D. Bensimon, A. Horovitz, G. Haran, *Proc. Natl. Acad. Sci. U.S.A.* **2012**, *109*, E1437-E1443.
[15] R. El-Sayed, K. Bhattacharya, Z. Gu, Z. Yang, J. K. Weber, H. Li, K. Leifer, Y. Zhao, M. S. Toprak, R. Zhou, B. Fadeel, *Sci. Rep.* **2016**, *6*, 21316.
[16] A. Y. Louie, T. J. Meade, *Chem. Rev.* **1999**, *99*, 2711-2734.
[17] M. Xu, S. Yuan, X.-Y. Chen, Y.-J. Chang, G. Day, Z.-Y. Gu, H.-C. Zhou, *J. Am. Chem. Soc.* **2017**, *139*, 8312-8319.

[18] R. Rauh, A. Diakov, A. Tzschoppe, J. Korbmacher, A. K. Azad, H. Cuppens, J.-J. Cassiman, J. Dötsch, H. Sticht, C. Korbmacher, *J. Physiol.* **2010**, *588*, 1211-1225.
[19] C. Stehlik, *Arthritis Rheum.* **2009**, *60*, 3524-3530.
[20] B. S. Sandanaraj, D. R. Vutukuri, J. M. Simard, A. Klaikherd, R. Hong, V. M. Rotello, S. Thayumanavan, *J. Am. Chem. Soc.* **2005**, *127*, 10693-10698.
[21] S. S. Chou, B. Kaehr, J. Kim, B. M. Foley, M. De, P. E. Hopkins, J. Huang, C. J. Brinker, V. P. Dravid, *Angew. Chem. Int. Ed.* **2013**, *52*, 4160-4164.
[22] R. Hong, N. O. Fischer, A. Verma, C. M. Goodman, T. Emrick, V. M. Rotello, *J. Am. Chem. Soc.* **2004**, *126*, 739-743.
[23] M. De, S. S. Chou, V. P. Dravid, *J. Am. Chem. Soc.* **2011**, *133*, 17524-17527.
[24] B. Zhang, Y. Xing, Z. Li, H. Zhou, Q. Mu, B. Yan, *Nano Lett.* **2009**, *9*, 2280-2284.
[25] K. Sarkar, M. Paul, P. Dastidar, *Chem. Commun.* **2016**, *52*, 13124-13127.
[26] K. Kano, Y. Ishida, *Chem. Asian J.* **2008**, *3*, 678-686.
[27] P. B. Sigler, B. A. Jeffery, B. W. Matthews, D. M. Blow, *J. Mol. Biol.* **1966**, *15*, 175-192.
[28] H. Lineweaver, D. Burk, *J. Am. Chem. Soc.* **1934**, *56*, 658-666.
[29] R. A. Copeland, Enzymes: A Practical Introduction to Structure, Mechanism, and Data Analysis; Wiley-VCH: New York, **2000**; Chapter 8, 268−282.

10.1002/chem.201802376

WILEY-VCH

Entry for the Table of Contents

COMMUNICATION

As much as ~97 % inhibition of the activity of a digestive enzyme α-chymotrypsin was achieved by 2D exfoliated nano-sheets of a Cu(II) coordination polymer (CP1) designed by considering the structure of the active site of the enzyme as well as its mode of action.

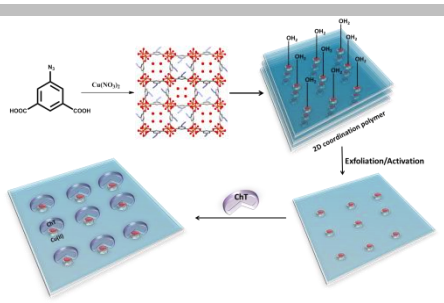

*Koushik Sarkar and Parthasarathi Dastidar**

Page No. – Page No.
A Cu(II) coordination polymer based exfoliated nano-sheet inhibits α-chymotrypsin